ORIGINAL PAPER

PGA distributions and seismic hazard evaluations in three cities in Taiwan

Jui-Pin Wang · Su-Chin Chang · Yih-Min Wu · Yun Xu

Abstract   This study first presents the series of peak ground acceleration (PGA) in the three major cities in Taiwan. The PGAs are back-calculated from an earthquake catalog with the use of ground motion models. The maximums of the 84th percentile (mean + one standard deviation) PGA since 1900 are 1.03, 0.36, and 0.10 g, in Taipei, Taichung, and Kaohsiung, respectively. Statistical goodness-of-fit testing shows that the series of PGA follow a double-lognormal distribution. Using the verified probability distribution, a probabilistic analysis was developed in this paper, and used to evaluate probability-based seismic hazard. Accordingly, given a PGA equal to 0.5 g, the annual exceedance probabilities are 0.56, 0.46, and 0.23 % in Taipei, Taichung, and Kaohsiung, respectively; for PGA equal to 1.0 g, the probabilities become 0.18, 0.14, and 0.09 %. As a result, this analysis indicates the city in South Taiwan is associated with relatively lower seismic hazard, compared with those in Central and North Taiwan.

Keywords   Probability-based seismic hazard · Double-lognormal distribution · Three major cities in Taiwan

J.-P. Wang (✉) · Y. Xu
Department of Civil and Environmental Engineering, The Hong Kong University of Science and Technology, Kowloon, Hong Kong
e-mail: jpwang@ust.hk

S.-C. Chang
Department of Earth Sciences, The University of Hong Kong, Pokfulam, Hong Kong

Y.-M. Wu
Department of Geosciences, National Taiwan University, Taipei, Taiwan

1 Introduction

Taiwan is located in the western portion of the circum-Pacific seismic belt, and the area is one of the most seismically active regions in the world. Thus, the Taiwan Island has a high rate of crustal deformation, and has been repeatedly struck by catastrophic earthquakes. The Chi-Chi earthquake in 1999 was the recent catastrophic event that caused thousands of casualties and countless loss in economy. Local researchers have spent lots of efforts on a variety of earthquake-related studies, in a hope to develop local earthquake-resistant designs, and to mitigate potential earthquake hazards in Taiwan. The Central Geological Survey, Taiwan, has launched the investigation into active faults on the island, and the results have been published with periodical updates (Lin et al. 2008, 2009). Other studies, including the probabilistic seismic hazard analysis (PSHA) (Cheng et al. 2007) and earthquake early warning (Wu and Kanamori 2005a, b), have also been conducted for the region of Taiwan.

Earthquakes are believed to be unpredictable, or the predictions of the exact time, location, and size of next catastrophic earthquakes are impossible (Geller et al. 1997). However, the community agrees that seismic hazard analysis is a logical and practical approach (Geller et al. 1997), and can be used for developing the earthquake-resistant designs of engineered structures. PSHA, developed in the late 1960s (Cornell 1968), is one of the methods with a few case studies being performed for some regions in the past decade (e.g., Cheng et al. 2007; Sokolov et al. 2009). Its growing popularity is also reflected by the fact that a couple technical guidelines have used it for developing the earthquake-resistant designs of critical structures (U.S. NRC 2007; IAEA 2002). Although PSHA has become the standard procedure in a site-specific design, the legitimacy in its framework has been under debate (Krinitzsky 1993a, b; Bommer 2002, 2003; Castanos and Lomnitz 2002). On the other hand, a few other probability-based approaches have been also developed for evaluating earthquake potentials (Jafari 2010; Wang et al. 2011).

This study aims to evaluate the seismic hazard in Taiwan by a new probabilistic procedure statistically analyzing the distribution of peak ground motions (PGA) in the past 110 years. The seismic hazards in three major cities in the North (Taipei), Central (Taichung), and South (Kaohsiung) Taiwan are evaluated by the approach, through a reliable earthquake catalog since 1900 and local ground motion models reported in the literature.

2 Distributions of semi-observed ground motion

2.1 Semi-observed ground motion

During an earthquake, the ground motion at a site can be measured by modern instrumentation. But unlike an earthquake catalog, there is yet a ground motion catalog available for a given location. Since earthquake-induced ground motion at the site of interest can be estimated by an attenuation relationship, a series of site-specific ground motions can be established from an earthquake catalog along with suitable ground motion models. Since they are not directly measured or observed, we consider them the semi-observed ground motions in this study.

2.2 Ground motion models

A ground motion model provides a predictive relationship between an earthquake and its ground motion at a site (Kramer 1996). Its general expression is as follows:

$$\ln Y = f(\theta_1, \ldots, \theta_n) = f(\mathbf{\Omega}); \quad 4\sigma_{\ln Y} = \sigma^* \tag{1}$$

where Y denotes ground motion; $\theta_1, \ldots, \theta_n$ denote earthquake variables, for example, magnitude, distance; $\mathbf{\Omega}$ denotes the set of earthquake variables $\theta_1, \ldots, \theta_n$; f denotes a predictive function. The model uncertainty ($\sigma_{\ln Y}$) is prescribed by a constant σ^* during its development. It is worth noting that the logarithm of ground motion ($\ln Y$) follows a normal distribution, with its mean ($\mu_{\ln Y}$) and standard deviation ($\sigma_{\ln Y}$) equal to $f(\mathbf{\Omega})$ and σ^*, respectively (Kramer 1996). As a result, the relationship between Z (standard normal variate), Y, $f(\mathbf{\Omega})$, and σ^* is as follows (Ang and Tang 2007):

$$
\begin{aligned}
Z &= \frac{\ln Y - \mu_{\ln Y}}{\sigma_{\ln Y}} \\
&\Rightarrow \ln Y = Z \times \sigma_{\ln Y} + \mu_{\ln Y} \\
&\Rightarrow \ln Y = Z \times \sigma^* + f(\mathbf{\Omega}) \\
&\Rightarrow Y = \exp(Z \times \sigma^* + f(\mathbf{\Omega}))
\end{aligned}
\tag{2}
$$

Since $\ln Y$ follows a normal distribution, its 50th and 84th percentiles are corresponding to Z equal to 0 and 1, respectively. With 0 and 1 being substituted into Eq. 2, the 50th and 84th percentiles of Y for a given $f(\mathbf{\Omega})$ and σ^* become:

$$Y_{50} = \exp(f(\mathbf{\Omega})) \tag{3}$$

$$Y_{84} = \exp(\sigma^* + f(\mathbf{\Omega})) \tag{4}$$

2.3 Magnitude and distance thresholds

Similar to PSHA, magnitude and distance thresholds are the two parameters associated with the following analytical procedure. The earthquakes with a small magnitude or large source-to-site distance are unlikely to cause structural damage, and those will be not considered in seismic hazard assessments. In this study, a "featured" earthquake is defined as one with large magnitude and small source-to-site distance, potentially resulting in a destructive ground motion at a site of interest. In the following analyses, six sets of magnitude and distance thresholds (M_0, R_0) were used, which are (5.5 M_w, 100 km), (5.5 M_w, 150 km), (5.5 M_w, 200 km), (6.0 M_w, 150 km), (6.0 M_w, 200 km), and (6.5 M_w, 250 km). It should be noted that the thresholds are in accord with the evaluation of earthquake potentials in the city of Tehran, Iran (Jafari 2010).

2.4 Inputs: earthquake catalog, ground motion model, etc

The earthquake catalog used in analyzing the distribution of annual maximum earthquake magnitudes around Taiwan (Wang et al. 2011) was adopted in this study. Figure 1 shows the spatial distribution of more than 50,000 earthquakes since 1900. The catalog was declustered, and the earthquakes were recorded in local magnitude M_L. The ground motion models used in the recent PSHA studies for Taiwan were also used (Cheng et al. 2007). Table 1 summarizes the four ground motion models for PGA estimation, and each of them was used with an equal weight to consider the (epistemic) uncertainty. Because the magnitudes in ground motion models and the earthquake catalog are different, an empirical relationship is needed for the conversion between moment magnitude M_w and local magnitude M_L as follows (Wu et al. 2001):

$$M_L = 4.533 \times \ln(M_w) - 2.091 \tag{5}$$

2.5 The 50th PGA in the three major cities in Taiwan

As an example, Fig. 2 shows the distributions of the 50th PGAs near Taipei, calculated from the 128 featured earthquakes given the threshold equal to (6.0 M_w, 200 km). The mean, coefficient of variation (COV), and maximum of the 50th PGA are 22.4 gal, 235 %, and 579 gal, respectively. The maximum is associated with the earthquake in 1909 with its magnitude and source-to-site distance of 7.9 M_w and 5.5 km, respectively.

Figure 3 shows the statistics of the 50th PGAs near the three cities under the six thresholds. It was found that the mean and COV show a negative correlation. In contrast, a positive correlation was observed between earthquake rate and COV. The possible cause for the positive correlation observed is suggested as follows. That is, the higher likelihood of extreme occurrences is expected given more events. With an extreme PGA, the variation of back-calculated PGA will increase significantly. On the other hand, the negative correlation between PGA's mean and COV is expected owing to the definition of COV being standard deviation$/_\text{mean}$.

In addition, the numbers of featured earthquakes and the mean values of the 50th PGA in Taipei and Taichung are found comparable, and both are higher than those of Kaohsiung. The higher rate in Taipei and Taichung results from their location being closer to the subduction zone located in the eastern offshore, where a high concentration of earthquakes is observed in Fig. 1. In contrast, the city in the south is subject to a relatively lower earthquake threat in terms of earthquake frequency. It was also found that except for Kaohsiung, the maximum PGA is independent of the six thresholds. With the threshold (6.0 M_w, 250 km) being used in Kaohsiung, the maximum is 53 gal associated with

Fig. 1 Spatial distribution of the seismicity around Taiwan since 1900 (Wang et al. 2011)
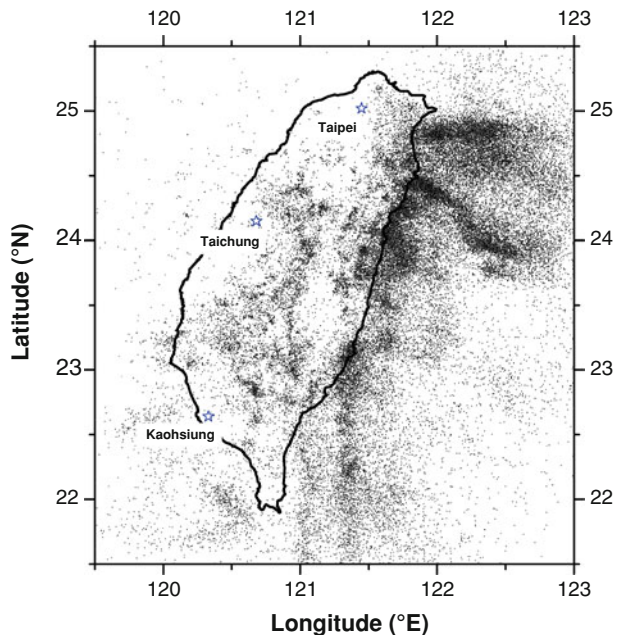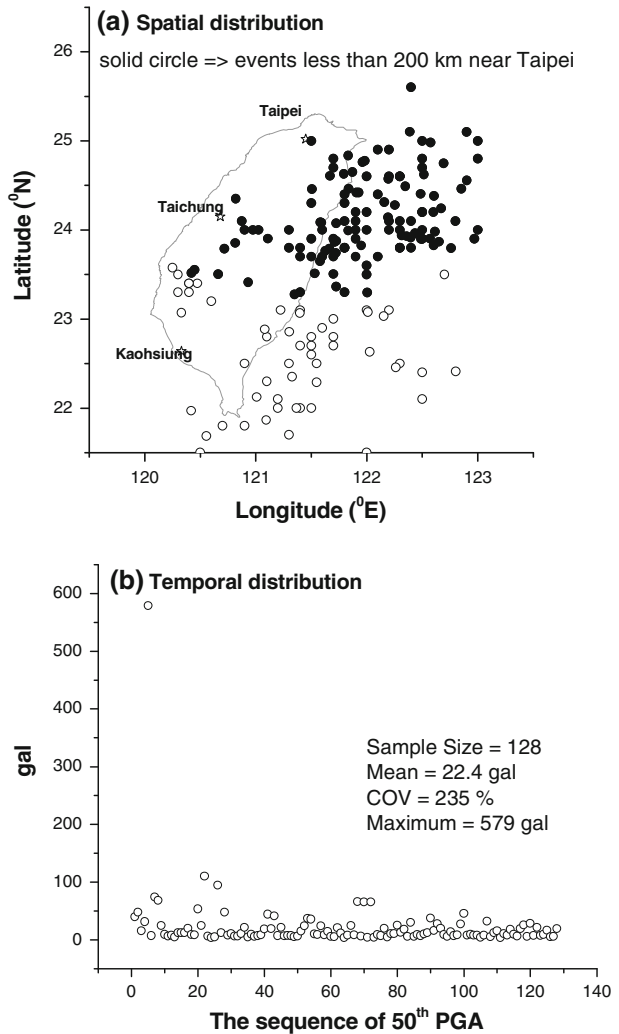
Table 1 Ground motion models used in this study (Cheng et al. 2007)

Description	PGA attenuation relationship	$\sigma_{\ln y}$
Hanging wall, rock, crustal	$\ln y = -3.25 + 1.075\, M_w - 1.723\, \ln[R + 0.156\, \exp\,(0.62391\, M_w)]$	0.577
Hanging wall, soil, crustal	$\ln y = -2.80 + 0.955\, M_w - 1.583\, \ln[R + 0.176\, \exp\,(0.603285\, M_w)]$	0.555
Foot wall, rock, crustal	$\ln y = -3.05 + 1.085\, M_w - 1.773\, \ln[R + 0.216\, \exp\,(0.611957\, M_w)]$	0.583
Foot wall, soil, crustal	$\ln y = -2.85 + 0.975\, M_w - 1.593\, \ln[R + 0.206\, \exp\,(0.612053\, M_w)]$	0.554

Fig. 2 128 back-calculated PGAs near Taipei since 1900 with the threshold of (6.0 M_w, 200 km): **a** spatial distribution and **b** the magnitudes of ground motions

magnitude and distance of 9.3 M_w and 228 km, respectively. For others, the maximum becomes 51 gal associated with magnitude and distance of 7.4 M_w and 75 km, respectively.
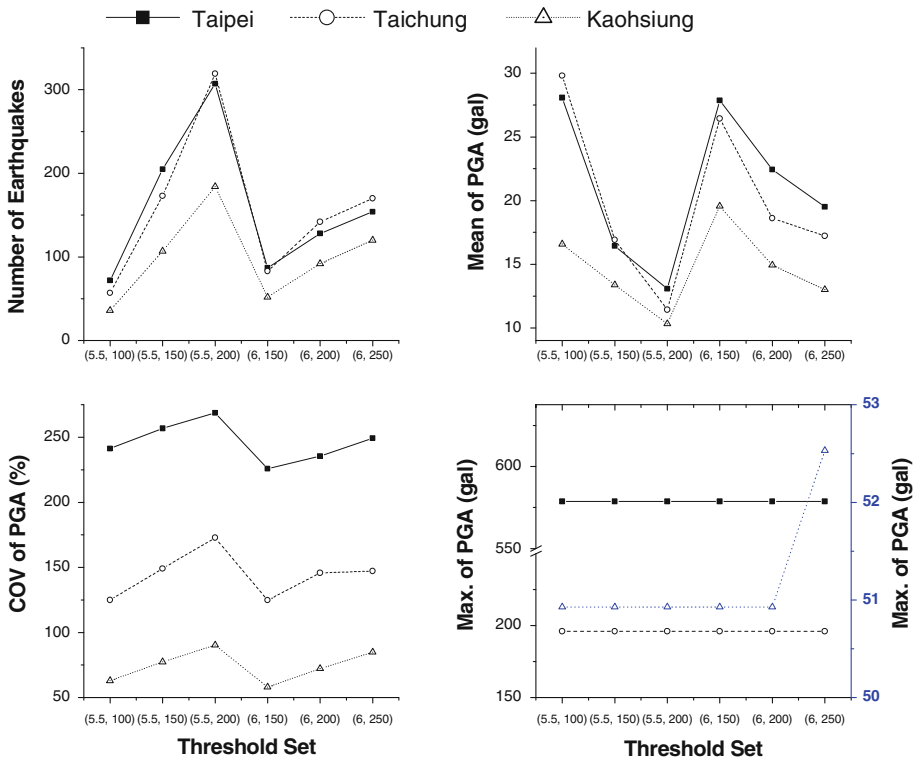
Fig. 3 Statistics of the 50th PGA in the three major cities in Taiwan, given six different magnitude and distance thresholds

2.6 The 84th PGA in the three major cities in Taiwan

The results shown in Fig. 3 are associated with the 50th PGA without considering the (aleatory) uncertainty σ^* of ground motion models. Using Eq. 4, Fig. 4 shows the statistics of the 84th PGA for the three cities. The means and maximums are increased due to the "plus one σ^*," with an approximately 70 % increase in mean and maximum being observed. However, the COVs of the 84th PGA remain a comparable level as the 50th percentile.

3 Probability distribution

3.1 Variable transformation

In Fig. 2b, the distribution of the 50th PGAs is highly asymmetrical. The widely used normal distribution is judged to be improper in modeling such an asymmetrical variable. In order to find a suitable probability model, other asymmetrical models, such as lognormal distribution, can be tested in a trial-and-error basis, or using variable transformation. Figure 5 shows that the series of (single-) logarithm and double-logarithm of PGAs in Fig. 2b demonstrating an increased level of symmetry in the transformed variables, especially for ln[ln(PGA)]. In other words, the normal distribution could become suitable in modeling the transformed variables.
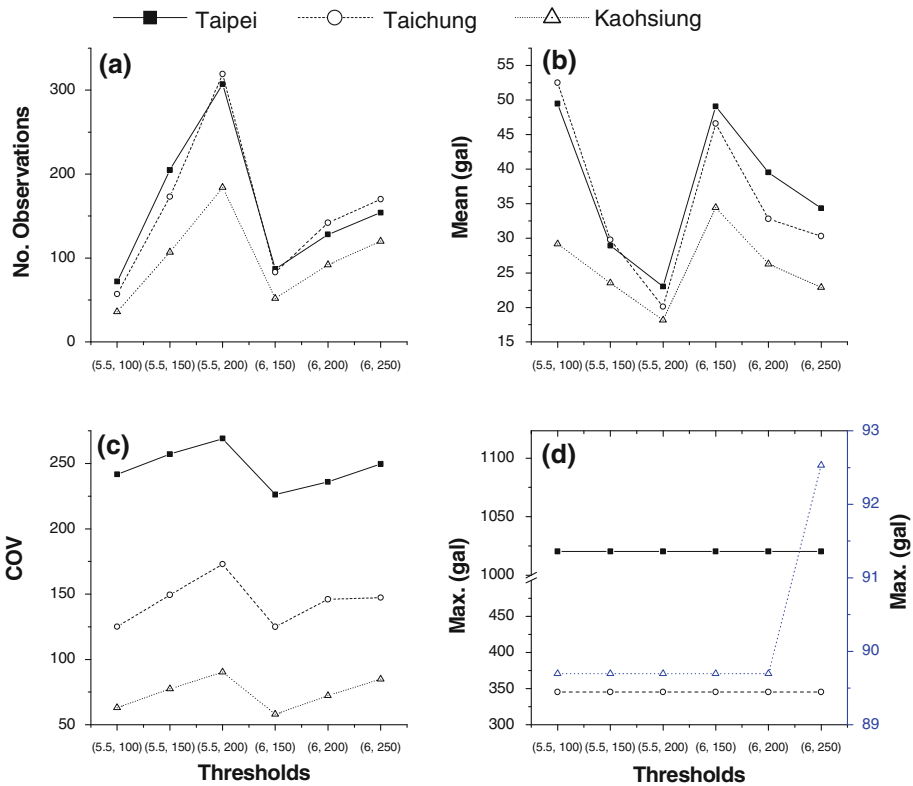
Fig. 4 Statistics of the 84th percentile PGA in the three major cities in Taiwan, with respect to six different magnitude and distance thresholds

3.2 Statistical goodness-of-fit testing

The Kolmogorov–Smirnov (K–S) test is one of the statistical approaches in goodness-of-fit testing (Ang and Tang 2007; Wang et al. 2011). Its essential is to compare the maximum difference between observational and theoretical cumulative probabilities. When the maximum difference is less than a critical value conditional to sample size and significance level in testing, the model is considered appropriate in simulating the variable from a statistical perspective. The mapping of observational cumulative probability $S_n(x)$ in the K–S test is as follows (Ang and Tang 2007; Wang et al. 2011):

$$S_n(x) = \begin{cases} 0 & x < x_1 \\ k/n & x_k \le x < x_{k+1} \\ 1 & x \ge x_n \end{cases} \tag{6}$$

where x_k denotes the k-th observation in an ascending order.

3.3 Appropriateness of double-lognormal distribution

Because the series of ln[ln(PGA)] were found symmetrical (Fig. 5b), the K–S test with 5 % level of significance was carried out in examining whether this transformed variable follows a normal distribution or the original variable follows a double-lognormal distribution.

Fig. 5 Distributions of
transformed PGA in Taipei:
a logarithm of 50th PGA and
b double-logarithm of 50th PGA

(a) Logarithm of 50th PGA, lnPGA$_{50}$

Sample Size = 128
Mean = 2.58 gal
COV = 33 %
Maximum = 6.36 gal

gal

The sequence of lnPGA$_{50}$

(b) Double logarithm of 50th PGA, ln(lnPGA$_{50}$)

Sample Size = 128
Mean = 0.90 gal
COV = 28 %
Maximum = 1.85 gal
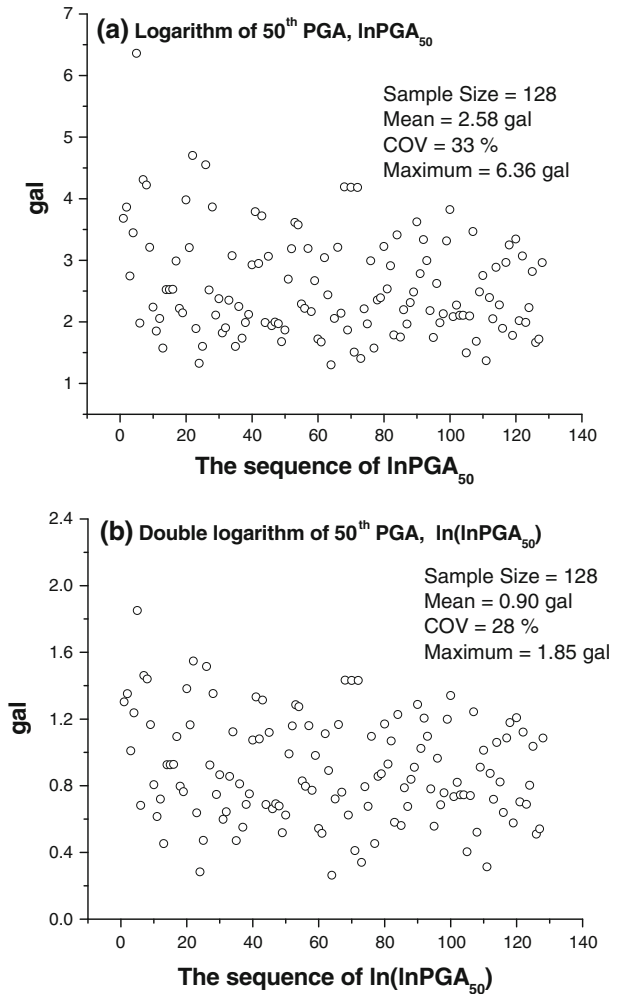
gal

The sequence of ln(lnPGA$_{50}$)

Figure 6 shows the maximum differences and critical values in different conditions for the 50th PGA. With the maximum difference less than the critical value, it indicates that the double-lognormal distribution is suitable in modeling PGA under the 18 conditions (three different cities and six different thresholds). Repeating the analysis for the 84th PGA, the results of testing are shown in Fig. 7. Similarly, the double-lognormal distribution was found appropriate, except for one scenario that the threshold (5.5 M_w, 150 km) was used in Taichung.

4 PGA exceedance probability by double-lognormal distribution

4.1 Seismic hazard

In earthquake engineering, seismic hazard, estimated by PSHA for example, is an estimate indicating a ground motion with its exceedance probability being identified (Cornell 1968;

Kramer 1996). Therefore, it is not an indication in physical damages caused by earthquakes, such as casualty, economic loss. For instance, PGA at 10 % exceedance probability within 50 years at Western and Eastern United States is around 0.6 g and less than 0.1 g, respectively (USGS 2008). Accordingly, site-specific earthquake-resistant designs intend to compensate different levels of seismic hazard, ensuring the same safety margin regardless of the location of a site.

4.2 At-least-one-event probability

The proposed approach with the use of the verified double-lognormal distribution was used to estimate the relationship between a given motion y^* and its probability, or simply being referred to as seismic hazard. In this study, the probability is the at-least-one-event likelihood, which is the probability indicating at least one PGA greater than a given PGA. The use of at-least-one-event probability is useful, considering the fact that a design is subject to failure as long as it experiences one motion exceeding its design motion. With the deterministic analysis used in failure assessment, the at-least-one-event probability can be related to the failure probability for an earthquake-resistant design. Take slope stability, for example, given a factor of safety equal to 1.0 with the use of y^* and its exceedance probability $\Pr(Y > y^*)$ equal to p^*, the failure probability of the slope must be equal to p^*, since any ground motion greater than y^* will result in a factor of safety less than 1.0, which dictates the scenario of failure.

4.3 Exceedance probability by double-lognormal distribution

With a random variable Y (PGA in this study) being verified to follow a double-lognormal distribution, the exceedance probability for a given y^* can be derived as follows:
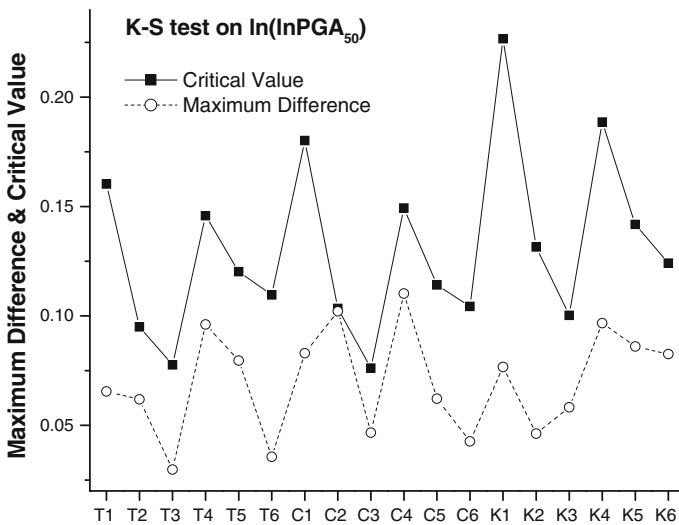

Fig. 6 K–S tests on the double-lognormal distribution in simulating the 50th PGA given 18 conditions, where *T*, *C*, and *K* denote Taipei, Taichung, and Kaohsiung, respectively, and *1–6* denote threshold sets (5.5 M_w, 100 km), (5.5 M_w, 150 km), (5.5 M_w, 200 km), (6.0 M_w, 150 km), (6.0 M_w, 200 km), and (6.0 M_w, 250 km), respectively
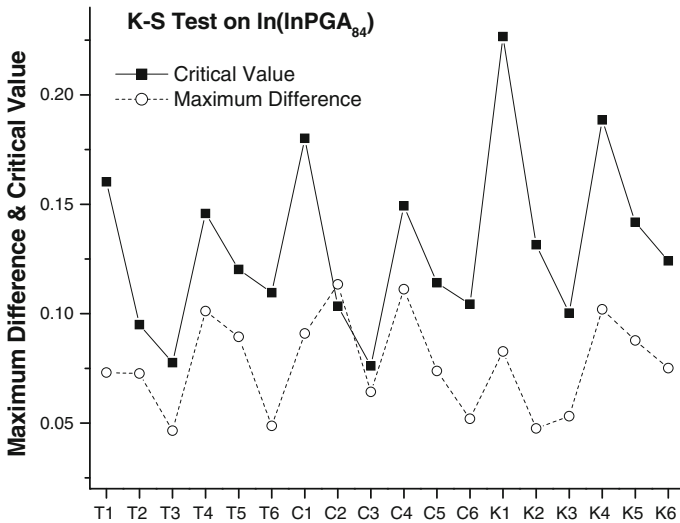
Fig. 7 K–S tests on the double-lognormal distribution in simulating the 84th PGA given 18 conditions

$$
\begin{aligned}
\Pr(Y > y^* | \mu_d, \sigma_d) &= \Pr(\ln(\ln Y) > \ln((\ln y^*)) | \mu_d, \sigma_d) \\
&= 1 - \Pr(\ln(\ln Y) \le \ln(\ln(y^*)) | \mu_d, \sigma_d) \\
&= 1 - \Phi\left(\frac{\ln(\ln(y^*)) - \mu_d}{\sigma_d}\right)
\end{aligned}
\tag{7}
$$

where μ_d and σ_d denote the mean and standard deviation (S.D.) of $\ln[\ln(Y)]$, respectively; Φ denotes the cumulative probability function of a standard normal variate. Equation 7 governs the exceedance probability in a single earthquake condition. Provided the variable is independently and identically distributed, the at-least-one-event exceedance probability becomes 100 % minus the probability of not a single PGA exceeding y^* in a multiple earthquake condition. Extended from Eq. 7, the exceedance probability for such a condition becomes:

$$
\Pr(Y > y^* | \mu_d, \sigma_d, n) = 1 - (\Pr(Y \le y^* | \mu_d, \sigma_d))^n
\tag{8}
$$

where n denotes the number of earthquake occurrences, and

$$
\Pr(Y \le y^* | \mu_d, \sigma_d) = \Phi\left(\frac{\ln(\ln(y^*)) - \mu_d}{\sigma_d}\right)
\tag{9}
$$

Equation 8 governs the exceedance probability in a n-earthquake condition. Owing to the random nature of earthquake occurrences in time, it is very unlikely that the same number of earthquakes recurs periodically. Therefore, the occurrence number (N) should be considered a random variable as well for better estimation in seismic hazard. With a Poisson distribution being recommended to simulate such a variable (Ang and Tang 2007; Jafari 2010), the probability density function for a given occurrence (n) with a mean rate equal to v is as follows (Ang and Tang 2007):

$$
P(N = n | v) = \frac{v^n \times e^{-v}}{n!}
\tag{10}
$$

Combining Eqs. 8 and 10, the exceedance probability becomes:

$$
\begin{aligned}
\Pr(Y > y^* | \mu_d, \sigma_d, v) \\
&= 1 - \sum_{n=0}^{\infty} \frac{v^n \times e^{-v}}{n!} \times \Pr(Y \le y^* | \mu_d, \sigma_d)^n \\
&= 1 - e^{-v} \left[\begin{array}{c} 1 + \dfrac{v \times \Pr(Y \le y^* | \mu_d, \sigma_d)}{1!} + \\ + \cdots + \dfrac{v^{\infty} \times P(Y \le y^* | \mu_d, \sigma_d)^{\infty}}{\infty!} \end{array} \right]
\end{aligned}
\tag{11}
$$

The term in the bracket is the Taylor expansion of $e^{v \times \Pr(Y \le y^* | \mu_d, \sigma_d)}$, so Eq. 11 becomes:

$$
\begin{aligned}
\Pr(Y > y^* | \mu_d, \sigma_d, v) &= 1 - e^{-v} e^{v \times \Pr(Y \le y^* | \mu_d, \sigma_d)} \\
&= 1 - e^{v \times (\Pr(Y \le y^* | \mu_d, \sigma_d) - 1)}
\end{aligned}
\tag{12}
$$

5 Results: seismic hazard assessments

With the use of Eqs. 8 and 12, this section shows the seismic hazard estimated by the new approach for the three cities in Taiwan. From the earthquake catalog, the parameters, μ_d, σ_d, and v, are calculated and summarized in Tables 2 and 3. Figures 8, 9, 10 show the annual hazard curves for following situations: (1) Y_{50} is used and N is considered a constant, (2) Y_{50} is used and N is considered a random variable, (3) Y_{84} is used and N is considered a constant, and (4) Y_{84} is used and N is considered a random variable, where Y_{50} and Y_{84} present the 50th and 84th percentiles of PGA, and N denotes the variable of earthquake occurrence in time. In each situation, six hazard curves are presented given respective magnitude and distance thresholds adopted. The respective hazard curves are different, but high seismic hazards are in general governed by those using the magnitude threshold of 6.0 M_w. The results also show that the hazard curves for Kaohsiung are highly conditional to thresholds in contrast to the other two cities.

Figure 11 shows the highest hazard curves under the four situations. The differences in seismic hazard between the two methods (Eqs. 8, 12) are negligible, indicating the variable type of occurrence number N having little impact on hazard curves. On the other hand, the use of the 84th PGA leads to high seismic hazard as expected, although the difference becomes less significant as a larger PGA is interested.

6 Best estimate seismic hazard

It has been shown that the hazard curves, especially for Kaohsiung, are affected by two factors: (1) magnitude thresholds and (2) Y_{50} or Y_{84} used in the analysis. In other words, the factors could dominate the level of seismic hazard, and how to determine the best factor would play a critical role in this analysis. Given the best factor that cannot be determined in a justifiable manner, we propose the best estimate hazard to be the envelope of those analyses using possible thresholds, in a conservative perspective to resolve the uncertainty in determining the best factors during analysis. Accordingly, Fig. 12 shows the best estimate curves for the three cities by enveloping the 24 possible scenarios. The estimations show a high seismic risk in Taipei, followed by the cities of Taichung and Kaohsiung. This

Table 2 Statistics of the 50th percentile ln[ln(PGA)]; μ_{d50} and δ_{d50} denote its mean and COV, respectively

Thresholds (M_w, km)	Taipei			Taichung			Kaohsiung		
	Rate (1/year)	μ_{d50} (gal)	δ_{d50} (%)	Rate (1/year)	μ_{d50} (gal)	δ_{d50} (%)	Rate (1/year)	μ_{d50} (gal)	δ_{d50} (%)
(5.5, 100)	0.65	1.01	23.7	0.52	1.05	25.6	0.33	0.96	19.5
(5.5, 150)	1.86	0.78	40.1	1.57	0.80	40.3	0.97	0.81	36.7
(5.5, 200)	2.79	0.64	59.9	2.90	0.57	72.3	1.67	0.63	63.5
(6.0, 150)	0.79	0.99	27.4	0.75	1.02	26.5	0.47	1.01	20.3
(6.0, 200)	1.16	0.90	34.6	1.29	0.84	40.4	0.84	0.86	34.8
(6.0, 250)	1.40	0.80	46.6	1.55	0.79	45.5	1.09	0.75	50.1

Table 3 Statistics of the 84th percentile ln[ln(PGA)]; μ_{d84} and δ_{d84} denote its mean and COV, respectively

Thresholds (M_w, km)	Taipei			Taichung			Kaohsiung		
	Rate (1/year)	μ_{d84} (gal)	δ_{d84} (%)	Rate (1/year)	μ_{d84} (gal)	δ_{d84} (%)	Rate (1/year)	μ_{d84} (gal)	δ_{d84} (%)
(5.5, 100)	0.65	1.20	16.8	0.52	1.24	18.3	0.33	1.16	13.4
(5.5, 150)	1.86	1.02	24.7	1.57	1.04	25.3	0.97	1.04	22.6
(5.5, 200)	2.79	0.92	32.4	2.90	0.86	36.4	1.67	0.91	33.3
(6.0, 150)	0.79	1.19	19.1	0.75	1.21	18.7	0.47	1.20	14.1
(6.0, 200)	1.16	1.11	22.8	1.29	1.06	25.6	0.84	1.08	22.1
(6.0, 250)	1.40	1.04	28.4	1.55	1.03	27.9	1.09	0.99	29.1

reflects the regional seismicity (Fig. 1), and the statistics of back-calculated PGA shown in Figs. 3 and 4. Given design motion equal to 0.5 g, the annual exceedance probabilities are 0.56, 0.46, and 0.23 % in Taipei, Taichung, and Kaohsiung, respectively. For an estimate of 1.0 g, the annual exceedance probabilities become 0.18, 0.14, and 0.09. At such ground motion levels, the annual exceedance probability in Taipei is approximately twice as large as that of the city in South Taiwan.

7 Discussion

7.1 Impact of catalog incompleteness

The incompleteness of an earthquake catalog would have a potential impact on seismic hazard assessment. A few studies were reported to adjust the catalog incompleteness before its use in relevant analyses (Kijko and Sellevoll 1990). The earthquake catalog used in this paper was reported for its incompleteness, especially in earlier years (Wang et al. 2011). But Wang et al. (2011) also verified that moderate earthquakes, say $M_w < 4.0$, are associated with high incompleteness in this catalog and that large earthquakes, say $M_w \geq 6.0$, are more or less complete with a steady rate being observed with time. Figure 13 shows temporal distributions for earthquakes in different magnitude thresholds. It was found that
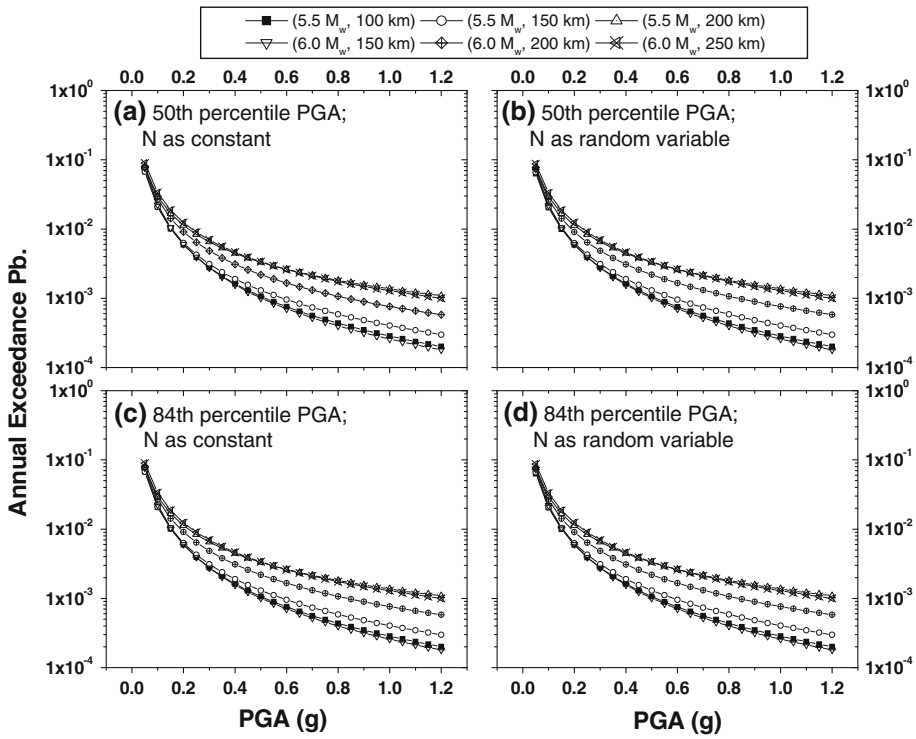
Fig. 8 Relationships between annual exceedance probability and PGA in 24 different conditions for Taipei

the distribution of large earthquakes does not increase with time (Figs. 13c, d). The variation is mainly associated with the random nature in earthquake occurrences.

Therefore, the impact of incompleteness on seismic hazard can be minimized in the new approach. Although the catalog inherits some degree of incompleteness for magnitude between 5.5 and 6.0 (Fig. 13b), their contribution to the best estimate hazard curve is negligible, since the envelope is mainly governed by those curves using $M_w \geq 6.0$ earthquakes, especially in high PGA ranges as shown in Figs. 8, 9 and 10.

7.2 Validation of results: empirical control

Klugel (2008) conducted a comprehensive review regarding existing seismic hazard analyses, and suggested that a reliable estimate of seismic hazard can somehow be validated by empirical controls given in some evidences such as historic seismicity. As mentioned, the maximums of the 84th PGA are 1.03 g (Taipei), 0.36 g (Taichung), and 0.10 g (Kaohsiung) in the past 110 years, and these PGAs are estimated with the annual exceedance probability equal to 0.9 % (=1/110), the reciprocal of the duration in the earthquake catalog. Through Fig. 12, the approach estimates the exceedance probabilities for these maximums around 0.13, 0.7, and 3 %, in Taipei, Taichung, and Kaohsiung, respectively, which are not significantly deviated from the empirical control (=0.9 %).
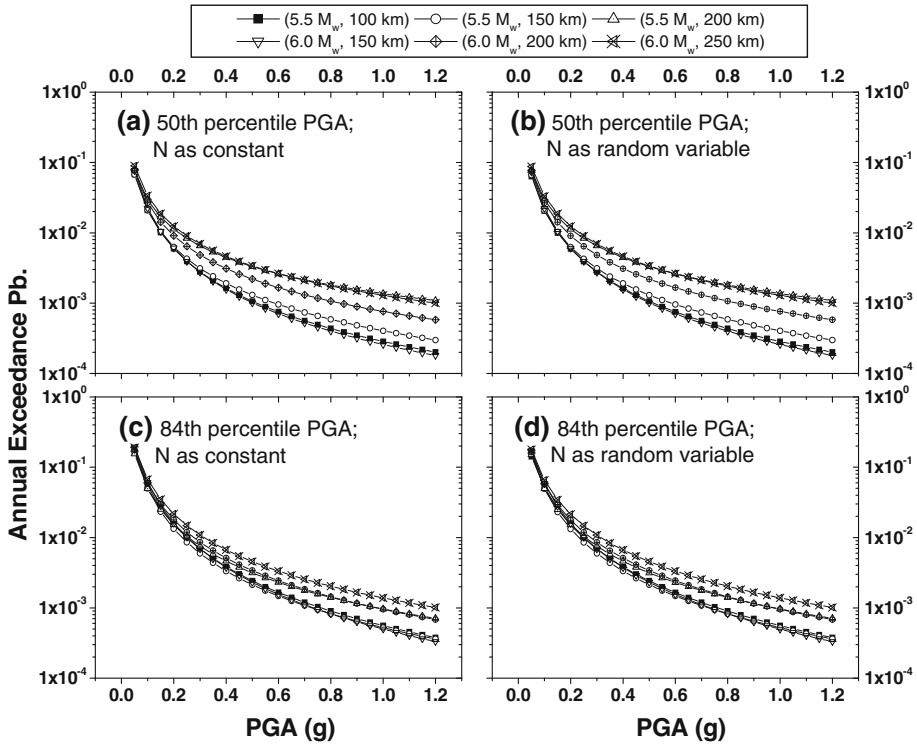
Fig. 9 Relationships between annual exceedance probability and PGA in 24 different conditions for Taichung

7.3 Limitation and recommendation

For statistical analyses, more samples can support a statistical relationship with more confidence, and the relationship can be less affected by a new sample which happens to be an outlier. Under the circumstance, the new approach is recommended for being used in actively seismic regions, such as Taiwan and Japan, where adequate earthquake observations are available.

Although the double-lognormal distribution in simulating PGA back-calculated from the earthquake catalog was verified to be appropriate, it must be noted that the verification is associated with the study region. When the approach is used in other regions, such as Japan, the assumption should better be verified beforehand. If the double-lognormal distribution in simulating PGA is still appropriate, the approach can be followed for seismic hazard assessments; otherwise, a new, proper probability distribution needs to be calibrated, and the probabilistic framework needs modification by replacing the double-normal distribution with the new model.

It is worth noting that the local ground motion models used in seismic hazard studies for Taiwan are conditional to magnitude and distance only. But it is believed that the depth of hypocenters can have an impact on resultant seismic hazard owing to different paths during wave propagation. As a result, this study can be further extended with the use of local,
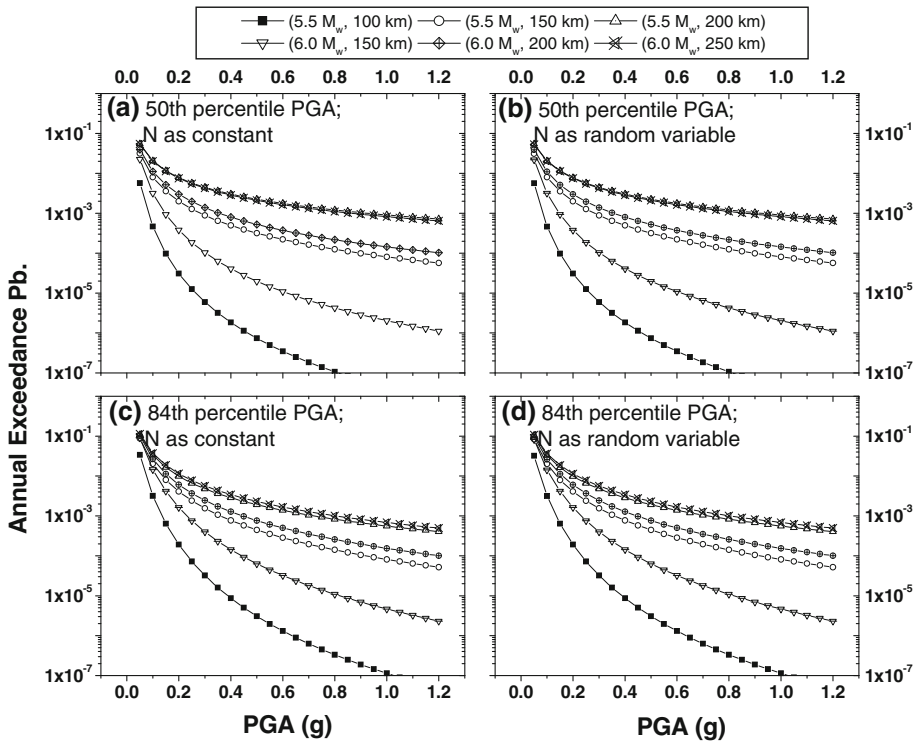
Fig. 10 Relationships between annual exceedance probability and PGA in 24 different conditions for Kaohsiung

reliable ground motion models capable of accounting for hypocenter depth in ground motion attenuation.

8 Conclusions

The series of PGA back-calculated from the earthquake catalog around three cities in Taiwan were presented in this paper. Since 1900, the maximums of the 84th PGA are 1.03, 0.36, and 0.10 g in Taipei, Taichung, and Kaohsiung, respectively. By statistical goodness-of-fit testing, the 50th and 84th PGAs in the three cities in Taiwan were found to follow a double-lognormal distribution. Given the verified probability distribution, a probabilistic procedure was developed to estimate the exceedance probability for a given PGA. In use of the method, the annual exceedance probabilities are 0.56, 0.46, and 0.23 % in Taipei, Taichung, and Kaohsiung, respectively, given PGA equal to 0.5 g; for PGA equal to 1.0 g, annual exceedance probabilities are 0.18, 0.14, and 0.09 %. This study shows that the seismic hazard in South Taiwan is relatively low compared to North and Central Taiwan.

Fig. 11 Highest seismic hazard curves among those using six different thresholds (shown in Figs. 8, 9, 10)
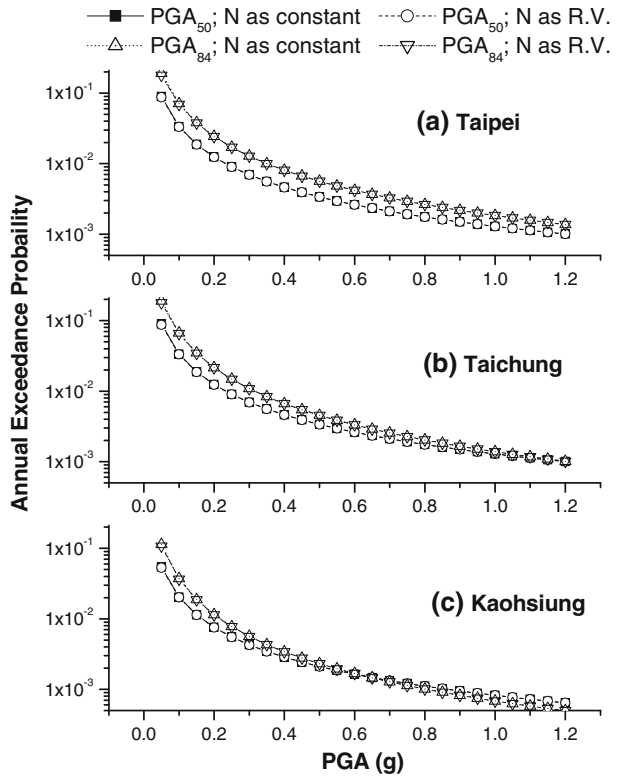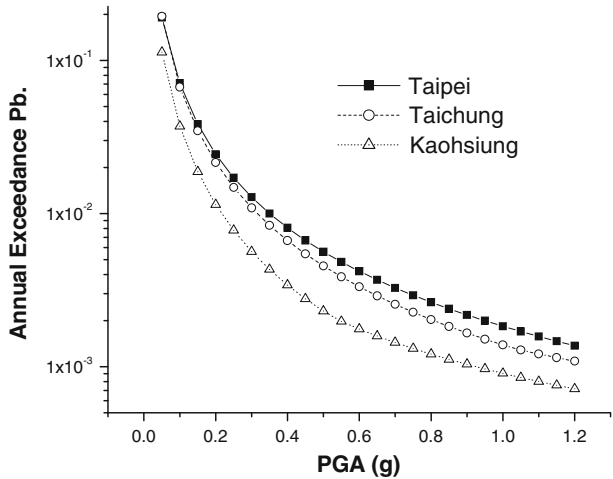

Fig. 12 Best estimate seismic hazard for the three cities in Taiwan; the curves are developed by enveloping 24 analyses in different conditions (shown in Figs. 8, 9, 10)
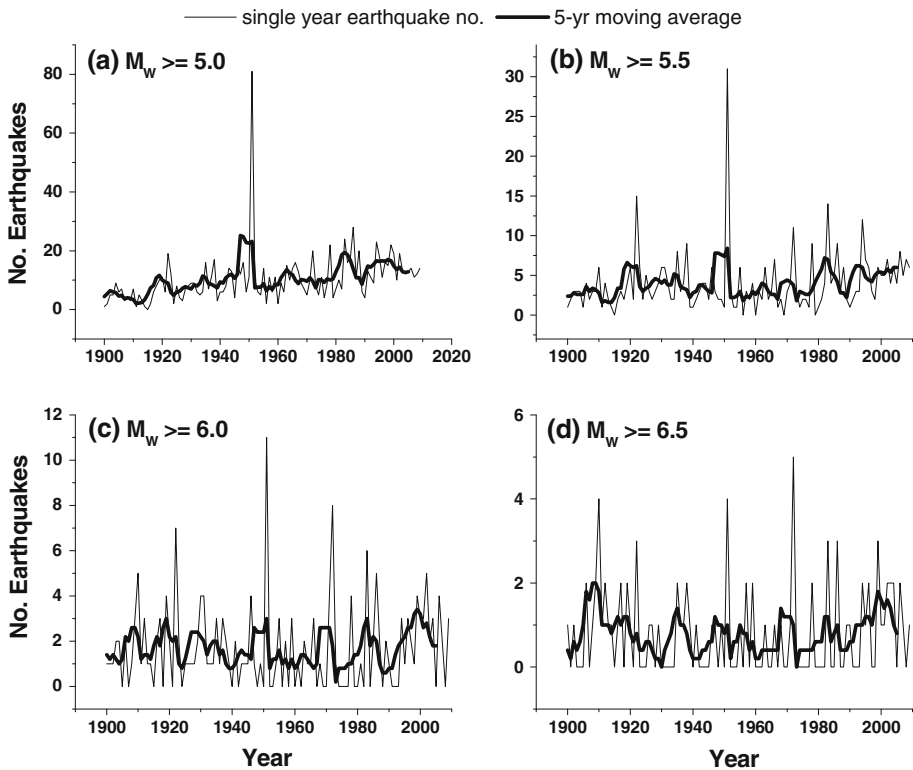
Fig. 13 Temporal distribution of earthquakes: **a** $M_w \geq 5.0$, **b** $M_w \geq 5.5$, **c** $M_w \geq 6.0$, and **d** $M_w \geq 6.5$

References

Ang AH, Tang WH (2007) Probability concepts in engineering: emphasis on applications to civil and environmental engineering, 2nd edn. Wiley, New Jersey, pp 96–99 (112, 293-295)

Bommer JJ (2002) Deterministic versus probabilistic seismic hazard assessment: an exaggerated and obstructive dichotomy. J Earthq Eng 6(Special Issue 1):43–73

Bommer JJ (2003) Uncertainty about uncertainty in seismic hazard analysis. Eng Geol 70(1–2):165–168

Castanos H, Lomnitz C (2002) PSHA: is it science? Eng Geol 66(3–4):315–317

Cheng CT, Chiou SJ, Lee CT, Tsai YB (2007) Study on probabilistic seismic hazard maps of Taiwan after Chi–Chi earthquake. J Eng Geol 2(1):19–28

Cornell CA (1968) Engineering seismic risk analysis. Bull Seismol Soc Am 58(5):1583–1606

Geller RJ, Jackson DD, Kagan YY, Mulargia F (1997) Earthquakes cannot be predicted. Science 275(5306):1616

IAEA (2002) Evaluation of seismic hazards for nuclear power plants. Safety Guide NS-G-3.3, International Atomic Energy Agency, Vienna

Jafari MA (2010) Statistical prediction of the next great earthquake around Tehran. Iran J Geodyn 49(1):14–18

Kijko A, Sellevoll MA (1990) Estimation of earthquake hazard parameters for incomplete and uncertain data files. Nat Hazards 3(1):1–13

Klugel JU (2008) Seismic hazard analysis—Quo vadis? Earth Sci Rev 88(1–2):1–32

Kramer SL (1996) Geotechnical Earthquake Engineering. Prentice Hall, New Jersey, pp 86–88 117-130

Krinitzsky EL (1993a) Earthquake probability in engineering-part 1: the use and misuse of expert opinion: the third Richard H. Jahns distinguished lecture in engineering geology. Eng Geol 33(3):219–231

Krinitzsky EL (1993b) Earthquake probability in engineering-part 2: earthquake recurrence and limitations of Guterberg-Richter b-values for the engineering of critical structures: the third Richard H. Jahns distinguished lecture in engineering geology. Eng Geol 36(1–2):1–52

Lin CW, Chen WS, Liu, YC, Chen PT (2009) Active faults of eastern and southern Taiwan. Special Publication of Central Geological Survey 23:178 (In Chinese with English Abstract)

Lin CW, Lu ST, Shih, TS, Lin WH, Liu YC, Chen PT (2008) Active faults of central Taiwan. Special Publication of Central Geological Survey 21:148 (In Chinese with English Abstract)

Sokolov VY, Wenzel F, Mohindra R (2009) Probabilistic seismic hazard assessment for Romania and sensitivity analysis: a case of joint consideration of intermediate-depth (Vrancea) and shallow (crustal) seismicity. Soil Dyn Earthq Eng 29(2):364–381

U.S. NRC (2007) Regulatory guide 1.208: A performance-based approach to define the site-specific earthquake ground motion. United States Nuclear Regulatory Commission, Washington

USGS (2008) National seismic hazard maps. United States Geological Survey, Virginia. http://earthquake.usgs.gov/hazards/

Wang JP, Chan CH, Wu YM (2011) The distribution of annual maximum earthquake magnitude around Taiwan and its application in the estimation of catastrophic earthquake recurrence probability. Nat Hazards 59(1):553–570

Wu YM, Kanamori H (2005a) Experiment on an onsite early warning method for the Taiwan early system. Bull Seismol Soc Am 95(1):347–354

Wu YM, Kanamori H (2005b) Rapid assessment of damaging potential of earthquakes in Taiwan from the beginning of P waves. Bull Seismol Soc Am 95(3):1181–1185

Wu YM, Shin TC, Chang CH (2001) Near real-time mapping of peak ground acceleration and peak ground velocity following a strong earthquake. Bull Seismol Soc Am 91(5):1218–1228